DOI: 10.31653/smf52.2026.125-151

дата першого надходження: 13.02.26
дата прийняття статті до друку після рецензування: 21.02.26
дата публікації: 05.05.26

Vychuzhanin V.V.[1], Vychuzhanin A.V.[2]

[1]ORCID: 0000-0002-6302-1832, [2]ORCID: 0000-0001-8779-2503

Odesa Polytechnic National University

DYNAMIC FAILURE RISK ASSESSMENT IN SHIP POWER PLANTS USING COGNITIVE DIGITAL TWINS

Statement of the problem in general terms. Modern ship power plants represent (SPPs) highly integrated complex technical systems (CTSs) operating under uncertainty, dynamic loads, and continuously changing environmental and operational conditions [1, 2]. The increasing level of automation and the transition toward autonomous and remotely operated vessels significantly intensify the requirements for reliability assessment, fault prediction, and real-time failure risk management.

In recent years, digital technologies for system monitoring and predictive maintenance [3, 4], including digital twins (DTs) [5], intelligent sensor platforms, and data-driven models, have been активно developed in various engineering domains [6, 7, 8]. Qi and Tao provided a comprehensive overview of DT applications and demonstrated their potential for lifecycle management and failure prediction in complex industrial systems [6]. Semeraro et al. conducted a systematic review of the DT paradigm and highlighted methodological gaps related to the formalization of cause-and-effect relationships and system-level integration [7]. Lv et al. analyzed the implementation of DTs in the marine industry and emphasized the early stage of methodological maturity and the lack of unified frameworks for maritime applications [8]. For complex cyber-physical systems, including power plants, reliability analysis and control architectures based on cyber-physical system technologies and industrial automation frameworks have been proposed [9]. However, such approaches are mainly architecture-oriented and do not provide dynamic risk assessment mechanisms or integrated failure propagation modeling. Recent research on engineering dynamics and DT modeling indicates the need for advanced simulation frameworks capable of capturing nonlinear system behavior and dynamic structural-functional interactions [10]. Nevertheless, existing approaches primarily focus on structural modeling and simulation accura-

cy and do not integrate cognitive models and real-time telemetry-driven risk assessment.

Therefore, a scientific and technical problem exists in developing integrated methods for dynamic assessment of structural and functional failure risks in SPPs based on the integration of DTs, cognitive modeling, and real-time telemetry data. This gap determines the relevance and necessity of the present study.

Analysis of recent studies and publications. The rapid development of Industry 4.0 technologies has significantly transformed approaches to monitoring, diagnostics, and prognostics of complex technical systems. Among these technologies, the concept of the DT has emerged as a key enabler for transitioning from traditional schedule-based maintenance toward intelligent condition-based and predictive maintenance strategies. By providing continuously updated virtual representations of physical assets, DTs support improved decision-making, enhanced reliability, and proactive risk mitigation.

In recent years, DTs have increasingly been recognized not only as monitoring tools but also as essential instruments for safety analysis and risk assessment. Zio and Miqueles emphasized that DT-based frameworks are becoming central in emergency management and reliability engineering, while also highlighting persistent challenges related to uncertainty quantification, model validation, and real-time risk propagation in interconnected systems [11]. These limitations are particularly critical in complex infrastructures, where failures may cascade across subsystems. The integration of DT technology into industrial and infrastructure projects introduces multidimensional risk dynamics. Ibrahim et al. provided a causal analysis of DT implementation, identifying governance, data reliability, and operational complexity as major factors influencing risk during DT adoption [12]. Similarly, comprehensive reviews of DT applications in infrastructure management underline the importance of combining IoT, AI, and simulation capabilities, yet point out that many existing studies remain focused on monitoring rather than adaptive risk-oriented decision support [13]. To address risk evaluation within DT environments, researchers have proposed extensions of classical reliability assessment methods. Li et al. demonstrated how improved FMEA techniques can be incorporated into DT project operation to strengthen risk identification and prioritization [14]. However, such approaches often remain limited to static evaluation schemes and do not fully capture the dynamic evolution of risks under real-time telemetry updates. Probabilistic DT frameworks

have recently gained attention as a means to support reliability-based maintenance optimization. For instance, probabilistic DT models have been successfully applied to offshore wind turbine maintenance planning, integrating reliability metrics with cost-aware decision-making [15]. Nevertheless, these methods are frequently domain-specific and do not directly address highly coupled safety-critical energy systems such as ship power plants, where structural dependencies play a dominant role. Emerging research further highlights the development of risk-aware DT paradigms. The concept of "Risk Twin" has been introduced to enable real-time visualization and control of structural risks, demonstrating the growing interest in DT-based risk analytics [16]. Risk-aware DT applications have also been explored in intelligent transportation and mobility systems, where real-time driver and infrastructure risk assessment becomes essential for operational safety [17]. In parallel, adaptive planning strategies for predictive DTs have been proposed, emphasizing the need for dynamic and self-updating risk management mechanisms [18]. Despite this progress, major gaps remain in the integration of cognitive reasoning and dynamic risk propagation modeling within DT architectures. Recent studies confirm that DT adoption for predictive maintenance is expanding rapidly, yet many implementations still lack robust mechanisms for holistic system-level risk assessment and explainable decision support [19]. Furthermore, security and trustworthiness issues, including cyber-physical vulnerabilities and AI-driven uncertainty, represent additional challenges for reliable DT deployment in critical infrastructures [20, 21].

These unresolved limitations are particularly evident in ship energy systems, where ship power plants consist of strongly interconnected subsystems such as fuel supply, lubrication, and cooling networks. Failures in such environments may propagate rapidly, requiring adaptive and cognitively informed risk assessment models beyond conventional diagnostics.

To address these challenges, the present study proposes a cognitive DT framework for the dynamic assessment of failure risks in ship power plants. By integrating cognitive simulation modeling with graph-based representations of structural and functional dependencies, the proposed approach enables real-time adaptive updating of risk indicators using telemetry-driven information. This methodology provides a practical foundation for improving operational safety, resilience, and proactive maintenance decision-making in complex maritime energy systems.

Setting the task. The objective of this paper is to develop and justify an integrated method for dynamic failure risk assessment of SPPs based

on a cognitive DT that combines DT technology and cognitive simulation modeling, using real-time telemetry data to quantitatively evaluate structural and functional risks and to predict cascading failure scenarios.

Presentation of the main research material. The analysis and assessment of failure risks in CTSs, in particular SPPs, in modern conditions require the integration of classical reliability assurance methods with modern approaches to digitalization. Stream analytics and intelligent diagnostic models form the information base for monitoring and predicting technical condition, expanding the capabilities of traditional methods. The basis remains a conceptual model that formalizes the interdependencies between elements, processes, and factors that influence failure risk. It is based on a systemic representation of the CTS as a set of interconnected elements interacting under conditions of uncertainty. In this approach, the risk of CTS equipment failure is considered as a function of the probability of failure and potential damage, and the assessment is carried out taking into account both structural and functional interrelationships between CTS subsystems. To formalize these interdependencies, a cognitive simulation model (CSM) is used, representing the system as a directed graph where nodes correspond to aggregates, subsystems and functional states, and arcs correspond to cause-and-effect relationships. This approach allows describing the structure of interaction and modelling the propagation of disturbances and failures through the hierarchy of elements. In the context of digital monitoring, diagnostics and forecasting of the technical condition of CTSs, CSM can use data from digital platforms and remote control systems to refine the parameters and relationships between elements. However, its main goal is to formalize the cause-and-effect relationships between failures, impacts and consequences, which allows for scenario analysis of risk development and forecasting of their temporal dynamics. The source of input data for CSM is digital monitoring platforms and the DT of the CTS. The DT accumulates the results of diagnostics, forecasting and assessment of the remaining service life of CTS equipment, forming a stream of parameters used to update the nodes and connections of the cognitive model. Thus, CSM does not duplicate the functions of DT, but uses it as a source of reliable data on the state of objects and external influences, thereby ensuring the realism of CTS equipment failure risk analysis scenarios. To ensure the practical applicability of CSM, it is important to establish a link between the abstract elements of the model and real operational data. In the context of digitalization, this role is performed by DT, which provides the cognitive model with reliable

information about the actual technical condition of the system. DT accumulates telemetry data streams and the results of diagnostic and predictive models (e.g., DCT, RUL estimates), forming a unified digital representation of the dynamic state of the object. This data is fed into the cognitive model in real time, where it is used to update cause-and-effect relationships, revise factor weights, and refine risk indicators. Thus, the integration of DT and CSM creates a closed-loop risk analysis cycle: from diagnostics to impact assessment and the formation of risk management recommendations.

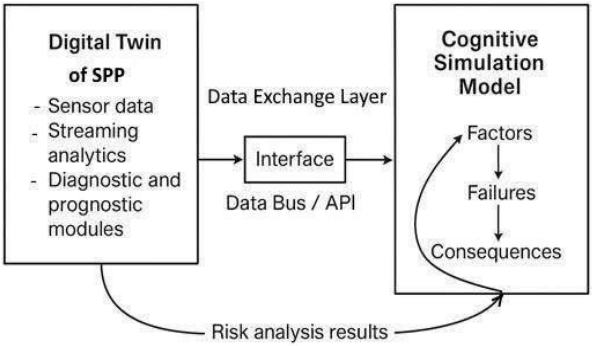

Fig. 1. Interaction between the DT and the CSM for risk assessment

Mechanism of dynamic linkage between DT and cognitive model. The conceptual interaction architecture presented in Figure 1 requires a robust mathematical formalization of the processes within the data exchange layer. To transform the CSM from a static graph into a dynamic predictive tool, a multi-stage algorithm for real-time weight recalculation is implemented. This algorithm ensures that telemetry data from the DT directly influences the propagation characteristics of the destructive modeling impulse (DMI).

1. Data transformation and normalization pipeline

The linkage between the physical state (DT) and the risk model (CSM) is established through a four-stage pipeline:

1.1. Diagnostic vector acquisition – the DT continuously streams a high-frequency telemetry vector $S(t)=\{p_1, p_2, ..., p_n\}$. For the ship's fuel system, these parameters include pump discharge pressure, fuel temperature, motor vibration levels, and filter differential pressure;

1.2. Standardized degradation mapping – to ensure comparability across different physical units, each parameter p_i is converted into a dimensionless degradation index $d_i \in [0, 1]$;

1.3. Sensor fusion and aggregation - multiple diagnostic signals affecting a single component are aggregated into a composite health index using importance weights;

1.4. Dynamic weight adaptation – the transition matrix of the CSM is updated, altering the "conductivity" of the graph for the DMI simulation.

2. Mathematical formalization of weight recalculation:

2.1. Parameter normalization

The degradation index d_i for each sensor is calculated based on its proximity to the operational limits:

$$d_i = \begin{cases} 0, \ if \ \ p_{fact} \ \ is \ with \ in \ noinal \ range \\ \dfrac{\left| p_{fact} - p_{nom} \right|}{p_{crit} - p_{nom}}, \ if \ \ p_{fact} \ \ exceeds \ p_{nom} \\ 1, \ \ if \ \ p_{fact} \geq p_{crit} \end{cases}$$

where p_{fact} is the current value, p_{nom} is the manufacturer's recommended setting, and p_{crit} is the safety shutdown threshold

2.2. The weight update function

The cognitive weight $\omega_{a(v)j}$, which represents the probability or intensity of failure propagation through an edge or node, is updated using a non-linear exponential function. This function mimics the "tipping point" behavior of mechanical systems where risk increases rapidly as limits are approached:

$$\omega_{a(v)j}\left(t+1\right) = \omega_{a(v)j}^{base} \cdot \exp\left(\alpha \sum_{i=1}^{k} \beta_{i,j} \cdot d_{i,j}\left(t\right) \right),$$

where $\omega_{a(v)j}\left(t+1\right)$ – is the updated weight of the *j*-th element (node or arc) at time *t*+1;

$\omega_{a(v)j}^{base}$ – is the initial topological weight based on system design and redundancy;

j – is the unique index of the component in the system graph;

i – is the index of a specific diagnostic sensor $\sum_{i=1}^{k} \beta_{i,j}$ linked to component *j*;

α – is the global sensitivity coefficient (controls how aggressively the model reacts to any degradation);

$\beta_{i,j}$ – is the local importance coefficient of the *i*- th sensor for the *j*-th component, satisfying $\sum_{i=1}^{k}\beta_{i,j}$

The integrated reliability indicator of CTS elements - technical risk - is a combination of the probabilities of occurrence of hazards of a certain class (P_{wi}) and the losses resulting from accidents and undesired events caused by technical imperfections or violations of the operational rules of technical systems (Y_{wi}):

$$R \equiv \left[\left(P_1, Y_1\right), \left(P_2, Y_2\right), ..., \left(P_{wi}, Y_{wi}\right) \right].$$

The probability assessment of a node (edge) failure in the CTS CSM is determined based on the Bayesian method of CTS analysis [22]:

$$P\left(C \mid D\right) \equiv \frac{P\left(D \mid C\right) \cdot P\left(C\right)}{P\left(D\right)},$$

where $P(C)$ – is the prior probability of hypothesis C of node (edge) failure;

$P(C|D)$ – is the probability of hypothesis *C* given event *D* occurs (posterior probability);

$P(D|C)$ – is the probability of event *D* given hypothesis *C* is true;

$P(D)$ – is the total probability of occurrence of event *D*

To evaluate the functional operability and the corresponding damage of a CTS, a normalizing impact (NI) is applied to the nodes and edges of the CTS CSM digraph. The NI is defined in accordance with the Birnbaum criterion [23]. The NI in terms of evaluating the functional operability of the system $F(t)$ and an individual edge (node) $f_{a(v)}(t)$ is defined as follows:

$$\Theta b_{a(v)}\left(i \mid t\right) = \frac{\partial F\left(t\right)}{\partial f_{a(v)}\left(t\right)}.$$

The evaluation of the CTS functional operability using NI is carried out in three stages. At the first stage, the operability of the CTS in a fully functional (fault-free) state is assessed. At the second stage, the sequential failure of individual elements and inter-element links (IL) of the CTS CSM is simulated, and the assessment of a partially faulty system is determined for each structural component (SC). At the third stage, quantita-

tive estimates of the functional damages of an element and IL are performed. The quantitative estimate of the functional damage of a CTS element under F (nominal operability), F_i (system operability under failure of the i-th element (v_i)) is determined as follows:

$$Y_{fV_i} = F - F_i.$$

Quantitative assessment of the functional damage of the subsystem under F_j – the operability of the system with the j-th subsystem being faulty (a_j):

$$Y_{fA_i} = F - F_j.$$

For the CTS CSM, the risk assessment of the failure of the affected vertex (edge) of the model is determined as the product of the probability values of failure of the vertex (edge) of the CTS CSM and the corresponding assessment of the functional damage of the affected vertices (edges) of the digraph. The CTS digraph $G(V,A)$ consists of n vertices (nodes) and m arcs (directed edges). The set of graph vertices is V– ($V=\{v_i\}$, $i=1,n$) The set of (ordered) pairs of vertices, called arcs (directed edges) of the graph, is A– ($A=\{a_j\}=\{v_i, w_j\}$, $j=1,m$), where vertex v is called the start, and w the end of the arc. The reliability value of the CTS aggregate corresponding to vertex v_i is determined by

$$v_i(t) = P_{vi}(t < T).$$

If it is possible to distinguish constructive or functional aggregates of the CTS, the graph vertices correspond to the structural aggregates of the system, and the graph edges correspond to the interconnections (IC). If it is difficult to distinguish aggregates, the graph vertices correspond to the system parameters, and the graph edges represent the cause-and-effect relationships between the parameters. Multiple edges may enter or leave a node. In this case, one speaks of a set of edges incident to a given node of the graph. Each edge is incident to two nodes located at its ends. The qualitative representation of the state of the CTS aggregates and ICs is expressed by a functional dependency between the states of the aggregates or ICs, as well as by a certain type of loading from external or internal influences. Assessments in emergency scenarios of structural and functional failure risk of the CTS, taking into account the interconnection and interaction of its elements, include the following stages:

1) identification of interconnection and interaction of SC within the hierarchy and topology of the CTS, taking into account the used resource of ESI (energy, substance, information);

2) construction and analysis of the CTS CSM;

3) assessment of structural and functional damages of the CTS;

4) assessment of structural and functional risks of the CTS.

State parameter set of CTS elements:

$$v = \left[F_{v,n}; F_{v,1}; a_{zi}; a_{zj}; H_m^v(t); K_{V.d.b} \right],$$

where $F_{v,n}$ – is the nominal operability of the element;

$F_{v,1}$ – is the operability of the element in the case of its partial loss;

a_{zi}, a_{zj} – is the incoming and outgoing influences for the CTS element;

i, j – is the ordinal number of the incoming and outgoing influence for the CTS element;

K, m – is the total number of incoming and outgoing influences for the IL element;

$H_m^v(t)$ – is the transfer coefficient of the change in the amplitude of the destructive modeling impulse (DMI);

$H_m^v(t) = \dfrac{m_{imp_r}^v(t+1)}{m_{imp_k}^v(t)}$, $m_{imp_k}^v(t)$, $m_{imp_k}^v(t=1)$ – is the value of the amplitude of the DMI at moments in time t and t+1;

$K_{V.d.b}$ – is the coefficient of the degree of damage of the element

State parameter set of the IC of the CTS:

$$a = \left[F_{a,n}; F_{a,1}; v; w; H_m^a(t); K_{A.d.b} \right],$$

where $F_{a,n.}$ is the nominal operability of the IC;

$F_{a,1}$ – is the operability of the IC under partial degradation;

z – is the type of ECI resource;

$H_m^a(t)$ – is the amplitude variation transmission coefficient IC

$H_m^a(t) = \dfrac{m_{imp_r}^a(t+1)}{m_{imp_k}^a(t)}$, $m_{imp_k}^a(t)$, $m_{imp_k}^a(t=1)$ is the value of the amplitude variation transmission of the DMI at moments in time t and t+1;

$K_{A.d.b}$ – is the coefficient of the damage degree of the IC

To assess the functional damage of the CTS, a normalizing influence is applied to the vertices and edges of the directed graph of the IC CTS. When assessing the structural damage of the CTS, it is assumed that the initial state of an element (CSM) corresponds to 0 if the DMI does not pass through the element (CSM), and to 1 if the IC passes through the element (CSM). Resetting the state values of the elements (IC) before

each subsequent iteration of DMI propagation through the IC is performed at. The influence of the DMI on a vertex (edge) of the directed graph of the CSM CTS at a discrete time moment *t* is defined as:

$$1-imp_j(t)=\frac{w_{a(v)j}(t)}{w_{a(v)j}(t-1)K_{V.d.b}K_{A.d.b}},$$

where $imp_j(t)$ – is the impulse vector for the edge with index *j*;

$w_{a(v)j}(t)$, $w_{a(v)j}(t-1)$ – is the weight value of the edge (vertex) at time moments *t*, *t*–1.

When passing through the IC from v_i vertex to vertex w_j, the impulses imp_j and imp_i are related by the relation:

$$imp_j(t+1)=imp_j(t)\cdot H_m^a(t).$$

When passing through a vertex from the *i*-th IC to the *j*-th IC, the impulses imp_j and imp_i are related as follows

$$imp_j(t+1)=imp_i(t)\cdot H_m^v(t).$$

The completion of DMI propagation (completion of the simulation cycle) over the directed graph is determined by the total residual energy of the impulses in the system. The simulation terminates when the sum of the magnitudes of all active impulses falls below a predefined sensitivity threshold ε:

$$S=\left[\sum_{j=1}^{M} imp_i(t)\right]<\varepsilon,$$

where *M* – is the total number of edges and nodes in the CSM;

$imp_i(t)$ – is the magnitude of the impulse at the *j*-th element at discrete time t;

ε –is the sensitivity threshold (convergence criterion), typically set to $\varepsilon=10^{-4}$ or determined by the specific precision requirements of the digital twin's diagnostic modules.

Introducing the ε threshold prevents infinite computation loops and accounts for "insignificant" disturbances that no longer have a measurable impact on the structural or functional risk of the system. This approach aligns the cognitive model with the discrete-time data processing intervals of the DT. The DMI is generated at a conventionally defined affected vertex (edge), propagates to subsequent vertices (edges), sequentially disabling the interconnected SC of the CSM. The degree of damage from

the DMI to an element (CSM) of the CTS is determined by the damage degree coefficient of the element (IC):

$$K_{V.d.b} = \frac{w_v(t+1)}{w_v(t)\cdot\left(1-m^{v}_{imp_k}(t)\right)};$$

$$K_{A.d.b} = \frac{w_a(t+1)}{w_a(t)\cdot\left(1-m^{a}_{imp_k}(t)\right)};$$

where $w_v(t)$, $w_a(t)$, $w_v(t+1)$,$w_a(t+1)$ – is the value of the weight of an element (CSM) at time moment before t and $t+1$ after the impact of the DMI

A gradation of damage degree coefficient values by the level of damaging influence of each element on the structure of the CSM is assumed as follows: greater than 0.7 – maximum emergency; from 0.7 to 0.3 – preemergency; less than 0.3 – non-emergency. The values of structural damages resulting from the affected *i*-th vertex, *j*-th edge of the directed graph for the total number of affected vertices (*b*), edges (*c*) of the CSM:

$$Y_{S(V_i)} = \frac{b}{N},\ Y_{S(A_i)} = \frac{c}{M}.$$

The quantitative assessment of structural damage from an affected vertex (edge) of the CSM CTS is determined by the damage due to loss of connectivity of the CTS topological structures as the ratio of the affected aggregates to the total number of aggregates (ICs) of the CTS under a single aggregate (IC) failure and unobstructed propagation of the CSM through the CTS. The quantitative assessment of functional damage from an affected vertex (edge) of the IC CTS is determined by the damage due to the disruption of the functioning of aggregates (ICs) as the ratio of the CTS operability under its partial degradation by an aggregate (IC) to the nominal operability of the CTS. The failure risk assessment of an affected vertex (edge) of the IC CTS is defined as the product of the probability values of failure of the vertex (edge) of the IC CTS and the corresponding assessments of the structural and functional damages of the affected vertices (edges) of the directed graph.

To assess the functional damage of the CTS during the propagation of the harmful influence (HI) along the directed graph of the IC CTS, a matrix of values is formed, where each vertex and each edge is assigned a numerical value of the HI magnitude. Initially, all HI magnitude values are assumed equal to 1. During the propagation of the HI along the di-

rected graph, they change proportionally to the weighted values of the SC. Based on Birnbaum's criterion, the HI magnitude value for a selected vertex (edge) of the directed graph of the IC CTS is expressed as the product of the HI magnitude value for the preceding vertex (edge) and the weight value of the selected vertex (edge). For a vertex of the directed graph of the IC CTS, into which several edges enter, the HI magnitude values of

$$m_i(t) = \sum_{i=1}^{N} m_j(t);$$

$$m_i(t) = s_i \cdot m_t(t-1) + s_j \cdot m_t(t-1);$$

where s_i, s_j – is the weight of the *i*-th vertex and the *j*-th edge;

$m_i(t)$, $m_i(t–1)$ – is the magnitude of the HI passing through a vertex or edge at time moments *t* and *t*–1.

Quantitative assessments of functional damages are determined for: a failed element (v_i) as the difference between the nominal operability of the CTS and the operability of the system under failure of element (v_i); a failed IC (a_j) as the difference between the nominal operability of the CTS and the operability of the system under failure of IM (a_j). Structural failure risk of the *i*-th element and the *j*-th IC of the CTS is determined as

$$R_{sv_i} = Y_{sv_i} \cdot p_{v_i}(t);$$

$$R_{av_i} = Y_{sa_i} \cdot p_{a_i}(t);$$

where $p_{v_i}(t)$, $p_{a_i}(t)$ – is the are the probabilities of failure of the affected *i*-th element and *j*-th IC of the CTS

The structural failure risk of all elements and ICs of the CTS is

$$R_s^v = \sum_{ij}^{M} R_{sv_i} \cdot p_{v_i}(t);$$

$$R_s^a = \sum_{j}^{M} R_{sa_j} \cdot p_{a_j}(t).$$

The failure risk assessment under structural damage from the affected *i*-th vertex of the CSM CTS is

$$R_{sv_i} = k_{sv_i} \cdot p_{v_i}(t);$$

where k_{sv_i} – is the structural damage assessment from the affected th vertex of the CSM CTS

The failure risk assessment under structural damage from the affected *j*-th edge of the CSM CTS is

$$R_{sa_j} = k_{sa_j} \cdot p_{a_j}(t),$$

where k_{sa_j} – is the structural damage assessment from the affected *j*-th edge of the CSM CTS

The functional failure risk of the *i*-th element and *j*-th IC of the CTS is

$$R_{fv_i} = Y_{fv_i} \cdot p_{v_i}(t), \quad R_{fa_j} = Y_{fa_j} \cdot p_{a_j}(t).$$

The functional failure risk of all elements and ICs is

$$R^{v}_{Ffv_i} = \sum_{j}^{N} R_{fv_i} \cdot p_{v_i}(t),\ R^{a}_{Ffa_j} = \sum_{j}^{M} R_{fa_j} \cdot p_{a_j}(t).$$

The failure risk assessment under functional damage from the affected *i*-th vertex of the CSM CTS is

$$R_{fv_i} = k_{fv_i} \cdot p_{v_i}(t),$$

where k_{fv_i} – is the functional damage assessment from the affected *i*-th vertex of the CSM CTS

The failure risk coefficient under functional damage from the affected *j*-th edge of the CSM CTS is

$$R_{fa_j} = k_{fa_j} \cdot p_{a_j}(t),$$

where k_{fa_j} – is the functional damage assessment from the affected *j*-th edge of the CSM CTS

The probability of failure of elements and ICs is determined as

$$P_{v_i} = \frac{n_{v_i}}{\tau}, P_{a_j} = \frac{n_{a_j}}{\tau},$$

where P_{v_i} – is the probability of failure of the *i*-th element of the CTS;

P_{a_j} – is the probability of failure of the *j*-th IC of the CTS;

n_{v_i} – is the number of failures of the i-th element of the CTS;

n_{a_j} – is the number of failures of the *j*-th IC of the CTS;

τ – is the duration of statistical testing.

As a basis for determining the values of failure probabilities of elements and ICs of the CTS, the data from [24] may be used. The depend-

encies of the total structural and functional failure risks on the probabilities of complete and partial failures of all elements and ICs of the CTS servicing systems are determined by the total values of failure risks and the total probabilities of failure of elements and ICs of the CTS as

$$P_V = \frac{\sum_{i}^{N} P_{v_i}}{N}, P_A = \frac{\sum_{j}^{M} P_j}{M},$$

where P_V is the sum of failure probability values of the CTS elements;

P_A – is the total failure probability value of the CSM ICs;

N – is the number of CTS elements;

M – is the number of CTS ICs

To rank the obtained assessment of structural and functional failure risks of the CTS in emergency scenarios, the generalized Harrington desirability function is used to evaluate the failure risk level: 0–0.2 – minimal, the consequences of the accident are minimal and do not have a significant impact on the operation of the CTS; 0.2–0.37 – acceptable, the consequences of the accident are insignificant, allowing the CTS to operate without repair; 0.37–0.63 – maximal, the consequences of the accident allow CTS operation after repair works are performed; 0.63–1 – critical, the consequences do not allow the CTS to be operated.

Let us consider the functional diagram of the fuel system (Fig. 2) of the main engine of a SPP that uses diesel fuel and heavy fuel oil. It consists of storage tanks for diesel fuel (F1, FS1) and heavy fuel oil (F2, FS2), pumps F3 and FS3, heaters F4 and FS4, two heavy fuel oil separators (F6, FS6) and one diesel fuel separator (F5), separator pumps (F7, FS7, FN7), the diesel fuel service system (F8) and the heavy fuel oil service system (F9, FS9), circulation tank F10, booster pumps F11 and FS11, heater F12, bypass pipeline section F13, filters F14 and FS14, and a high-pressure pump. Redundancy is provided for pumps F3 and F11 (FS3 and FS11 respectively) and for separators F5 and F6 together with heaters F4 and pumps F7. Tanks F1, FS1, F2, FS2 and filters F14, FS14 can operate according to a continuously energized standby scheme. In the event of failure of any of the standby elements of the system, the main engine can be switched to diesel fuel. Expert and statistical assessment of SPP operation indicates that approximately 40% of failures are attributable to the diesel fuel equipment and fuel system, with the majority of failures being associated with breakdown of components operating under high pressure

conditions (high-pressure fuel pumps, injectors, etc.). Redundancy is provided for pumps F3 and F11 (FS3 and FS11 respectively) and for separators F5 and F6 together with heaters F4 and pumps F7. Tanks F1, FS1, F2, FS2 and filters F14, FS14 can operate according to a continuously energized standby scheme. In the event of failure of any of the standby elements of the system, the main engine can be switched to diesel fuel. Expert and statistical assessment of SPP operation indicates that approximately 40% of failures are attributable to the diesel fuel equipment and fuel system, with the majority of failures being associated with breakdown of components operating under high pressure conditions (high-pressure fuel pumps, injectors, etc.).

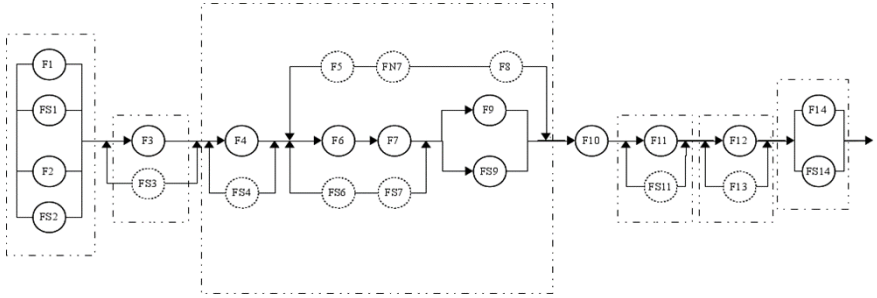

Fig. 2. Structural diagram of the ship power plant fuel system

The study of the effects of the DMI and HI on the CSM CTS was carried out in a developed software package based on the cross-platform Python language. To represent the input data of the elements and ICs when modeling emergency scenarios in the CSM CTS, the JSON format was used. The visualization of the graphs was performed using the Graphviz software product. MS Office and OpenOffice were used to analyze the research results. To test the method for assessing the structural and functional failure risks of the CTS in emergency scenarios (Fig. 3).

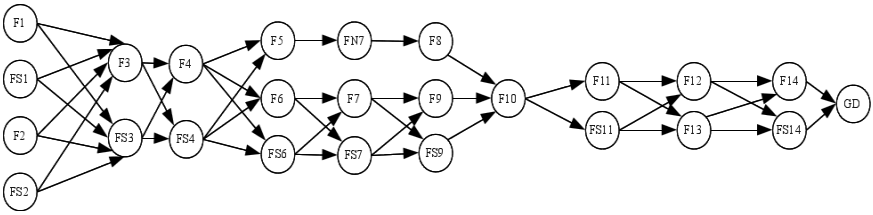

Fig. 3. Graph of the ship power plant fuel system

The modeling process for assessing the functional failure risks of the CTS elements and IMs was carried out in accordance with the algorithm shown in Fig. 4.

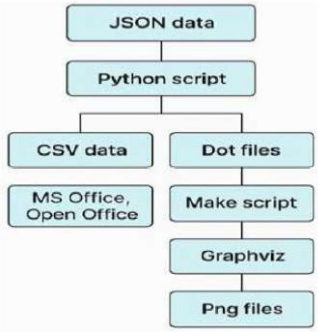

Fig. 4. Algorithm of the CTS operating conditions simulation process

To complement the workflow illustrated in Figure 4, it is necessary to specify the internal data structure of the JSON input file used by the Python simulation script. This specification acts as a standardized interface between the diagnostic telemetry gathered by the DT and the risk calculation engine of the cognitive model. Providing this schema is crucial for the scientific reproducibility of the study and its practical scalability.

Purpose of the JSON schema - the implementation of a structured data format serves three primary objectives:

- decoupling of systems - it separates the data acquisition layer (sensors/DT) from the analytical layer (CSM), allowing the risk model to be updated without altering the underlying telemetry hardware;
- dynamic reconfiguration – it enables the simulation engine to rebuild the system graph "on-the-fly" whenever a redundant component is activated or deactivated;
- standardization: it follows modern industrial IoT standards, facilitating integration with cloud-based monitoring platforms.

JSON data schema example - the system graph is represented as a structured object containing lists of nodes (components) and edges (inter-element connections).

```
{
  "system_id": "SPP_Fuel_System_v2",
  "nodes": [
    {
      "id": "F11",
```

"label": "Booster Pump",
"p_failure": 0.002,
"base_weight": 1.0,
"type": "mechanical"
},
{ "id": "F12", "label": "Fuel Heater", "p_failure": 0.005, "base_weight": 1.0 }
],
"edges": [
{
"source": "F10",
"target": "F11",
"resource": "fuel_flow",
"weight": 0.85
},
{ "source": "F11", "target": "F12", "resource": "fuel_flow", "weight": 0.90 }
]
}

Data field description:

nodes – a list of objects representing system components: id - unique identifier (e.g., "F10") corresponding to the functional scheme and the DTs sensor mapping; base_weight - the initial cognitive weight of the node, which is dynamically recalculated based on real-time telemetry updates;

edges – a list of directed arcs representing functional interdependencies: source / target: origin and destination nodes of the destructive modeling impulse (DMI) propagation; weight: the strength of the cause-and-effect relationship, determining the rate of failure propagation across the system topology.

This technical detail, combined with the methodology in Figure 4, provides a complete roadmap for deploying the risk assessment framework within a digital shipboard environment.

The recalculated weights are then compared against the Harrington desirability scale. If $w_{a(v)j}(t+1)>0.63$, the system automatically triggers a high-intensity DMI to simulate the "worst-case" cascading failure scenario starting from that specific component. The selection of nodes F10, F12, and GD as critical points in risk analysis is обусловлено their topological position in the graph and functional. To illustrate the algorithm, consider

the booster pump F11. The DT monitors two primary signals: discharge pressure (p_1) and vibration velocity (p_2).

Scenario 1. Nominal operation: telemetery: p_1=4.0 bar (Nominal: 4.0), p_2=2.5 mm/s (Nominal: 2.0, Crit: 7.0); Indices: d_1=0, d_2=0.1; result: w{F11} remains near its base value. Risk levels in Figures 4 and 6 remain in the "Safe" zone (<0.37).

Scenario 2. Impending cavitation or bearing wear: telemetery: pressure drops to 3.2 bar (d_1=0.4), vibration rises to 5.5 mm/s (d_2=0.7); aggregation: with β_1=0.4 and β_2=0.6, the composite degradation D=0.5. Impact: The weight of the outgoing edge F11→F12 more than doubles. In the next CSM iteration, the DMI propagates more aggressively through the fuel line, causing the functional risk R_{fa} for the entire SPP to cross the critical threshold of 0.63.

This detailed mechanism bridges the gap between low-level sensor data and high-level strategic risk assessment, allowing the SPP operator to visualize how a minor mechanical deviation in one pump increases the structural vulnerability of the entire power plant. The results of the calculated values of the structural and functional risk assessment for the vertices and edges of the CSM CTS are presented in Figs. 5-7. This section provides the simulation results for the structural and functional risks of the SPPs fuel system, based on the developed CSM. The results are interpreted according to Harrington's desirability scale, where values below 0.37 indicate a "Safe/Acceptable" zone, 0.37–0.63 represent a "Maximum/Pre-emergency" zone, and values above 0.63 denote a "Critical/Emergency" zone.

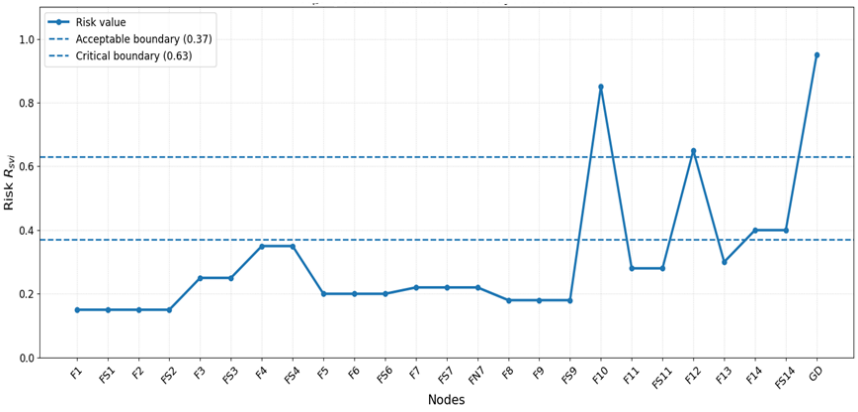

Fig. 5. Structural risk of system elements

Figure 5 illustrates the structural risk distribution across 25 nodes of the fuel system. The analysis reveals that nodes with built-in redundancy, such as the fuel transfer pumps (F3, FS3) and the separators (F5, F6, FS6), maintain risk levels within the "Safe" zone (R_{svi}<0.37). This confirms that the system's topological connectivity is robust in its initial stages. However, a significant spike is observed at node F10 (Circulation Tank), reaching a critical value of 0.85. As a non-redundant convergence point for both diesel and heavy fuel lines, F10 represents the most vulnerable bottleneck in the system's architecture. Similarly, the main engine node (GD) and the pre-filter heater (F12) exceed the 0.63 threshold. The results suggest that any failure at these "serial" points directly compromises the connectivity of the entire fuel supply chain, necessitating prioritized monitoring through the DT.

The risk assessment of the inter-element connections (Figure 6) shifts the focus from the components to the integrity of the transport channels. While the initial supply lines from the storage tanks (e.g., F1→F3) show minimal risk due to the abundance of alternative paths, the risk escalates sharply in the distribution manifold. The connections following the circulation tank (F10→F11) and the final delivery line to the engine (F14→GD) are identified as critical, with values exceeding 0.90. This indicates that the "structural health" of these specific pipeline segments is as vital as the performance of the pumps themselves. The high risk associated with the F12→F14 segment highlights the criticality of maintaining the thermal state of the fuel before filtration; a breach or blockage in this segment leads to immediate functional degradation of the SPP.

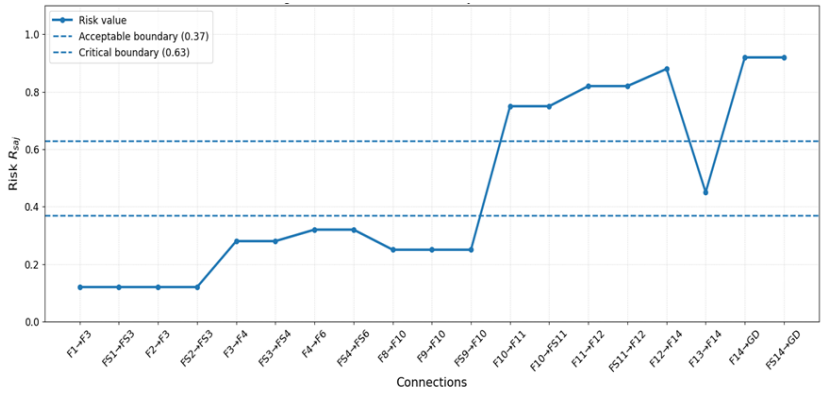

Fig.6. Structural risk of inter-element connections

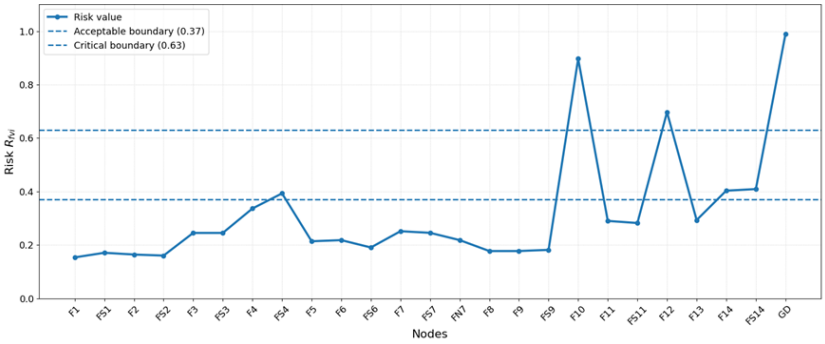

Fig.7. Functional risk of system components

Figure 7 presents the functional risk, which integrates structural connectivity with the severity of operational consequences. Following the statistical data cited in the study, which attributes approximately 40 % of failures to high-pressure fuel apparatus, the model shows elevated risk levels for the booster pumps (F11/FS11) and the main engine (GD). Unlike the purely structural analysis, the functional risk for node GD reaches its peak (0.95+), reflecting the catastrophic impact of a failure in fuel injection or atomization. The "Maximum risk" zone (0.37–0.63) encompasses the filtration unit (F14), suggesting that while the system might remain connected, a loss of filtering capacity significantly degrades the quality of the combustion process. These findings emphasize that risk management strategies in a Digital Twin environment must prioritize not just the existence of a flow path, but the operational parameters (pressure, purity, temperature) maintained by these critical components.

Based on the cognitive simulation of the SPPs fuel system, the most significant elements were identified and ranked by their impact on system reliability. Table 1 provides a quantitative summary of the structural and functional risks, categorized by the Harrington desirability scale.

The data in Table 1 clearly distinguishes between the "redundant safety" and "serial vulnerability" of the system:

critical zone (R>0.63): the GD, F10, and F12 elements represent the highest risk. The Main Engine (GD) shows the peak functional risk due to the statistical severity of high-pressure equipment failures. The Circulation Tank (F10) is identified as the primary structural bottleneck; its non-redundant nature makes it a single point of failure that compromises the entire fuel supply chain;

Table 1. Risk assessment summary for key fuel system components

Element ID	Component name	Structural risk (R_{svi})	Functional risk (R_{fvi})	Harrington scale level	Element ID
F10	Circulation tank	0.85	0.91	Critical	F10
F12	Final fuel heater	0.65	0.72	Critical	F12
F14/FS14	Fine filters (parallel unit)	0.40	0.52	Maximum	F14/FS14
F11/FS11	Booster pumps (redundant)	0.28	0.44	Maximum/ preemergency	F11/FS11
F4/FS4	Primary heaters	0.35	0.38	Maximum/ acceptable	F4/FS4
F3/FS3	Transfer pumps (redundant)	0.25	0.28	Acceptable	F3/FS3
F1/ S1	Diesel oil storage tanks	0.15	0.18	Minimal	F1/FS1

maximum risk zone (0.37–0.63): components such as F14 and F11 fall into this category. While they possess some level of redundancy or bypass capability (e.g., F13 for the heater or parallel filters), their degradation significantly increases the system's operational stress;

safe zone (R<0.37): redundant pumps (F3/FS3) and storage tanks show minimal risk levels, confirming that traditional hardware redundancy effectively mitigates topological vulnerabilities in the early stages of fuel processing.

This summary allows the DTs diagnostic system to prioritize alarm thresholds and maintenance schedules, focusing on the top three critical nodes to prevent cascading SPP failures. The developed method, validated through cognitive simulation modeling, makes it possible to identify the interrelated and interacting elements, interelement connections, as well as the degree of their influence on the assessment of the structural and functional risk of CTS failures, which in turn enables the automation of decision-making processes in emergency scenarios during CTS operation. The identified interdependencies and interactions of structural components within the hierarchy and topology of the CTS make it possible to determine the magnitude of the damaging influence of each system component in emergency scenarios on the structure of the CTS. The method’s procedures are easily formalized and transformed into a computational algo-

rithm and model for the assessment of structural and functional risks, which is important for CTS with a large number of elements and inter-element connections.

Discussion and comparative analysis of risk assessment methods. The effectiveness of the proposed integrated approach (DT-CSM) is best demonstrated by comparing it with traditional reliability assessment methods widely used in the maritime and industrial sectors, such as failure mode and effects analysis (FMEA) and fault tree analysis (FTA). The integration of DTs with CSMs provides a paradigm shift from static reliability estimation to dynamic risk management. Unlike FMEA/FTA, the DT-CSM method treats risk as a dynamic variable. By utilizing the algorithm described, the cognitive weights of the system graph are updated every few milliseconds based on actual telemetry (vibration, pressure, temperature). This allows the system to detect an escalating risk before a failure occurs. By employing the destructive modeling impulse (DMI) and the Harrington desirability scale, the proposed method identifies "gray zones"– conditions that are neither fully operational nor failed, but exhibit maximum structural risk. This granularity allows for condition-based maintenance (CBM) rather than fixed-interval maintenance. The shift from traditional methods to DT-CSM facilitates an evolution in how shipboard systems are maintained: reactive (traditional) – repair after failure (High risk for SPP); preventive (FMEA-based) – periodic maintenance based on average statistics (Leads to over-maintenance or missed early wear); predictive (DT-CSM-based) – maintenance triggered by the functional risk threshold R_{fvi}>0.63. This ensures that resources are focused on critical bottlenecks like node F10 or F12 only when real degradation is detected by the DT. A key differentiator of the CSM is its ability to model non-linear interdependencies. In an FTA, dependencies are hard-coded via logic gates. In the proposed CSM: feedback loops – the graph naturally represents circular dependencies (e.g., fuel heating affecting pump efficiency, which in turn affects heating stability); impulse propagation – the DMI mimics the physical flow of a disturbance. A vibration spike in pump F11 doesn't just "fail" that node; it weakens the "structural health" of all subsequent nodes (F12, F14, GD) proportionally to the weights of the arcs, providing a more realistic "heat map" of system vulnerability.

The proposed method leverages a modern software stack (Python, JSON, Graphviz), providing significant advantages in terms of computational efficiency and integration: computational complexity – while large fault trees suffer from exponential state space explosion, the impulse

propagation algorithm in the CSM operates with a complexity of O(N+M) per iteration, where N and M are the numbers of nodes and edges, respectively. This allows for near-instantaneous risk recalculation for systems with hundreds of components; data interoperability – the use of JSON-based configuration files allows for seamless integration with industrial IoT platforms and DT databases, unlike the static spreadsheets typical of FMEA

The comprehensive comparison of the technical, methodological, and operational attributes of the discussed is summarized in Table 2.

Table 2. Comparative summary

Feature	FMEA	FTA	Proposed DT-CSM Method
Data source	Expert judgment / history	Statistical probability	Real-time telemetry + DT
Update frequency	Monthly / yearly audits	Periodic updates	Continuous (ms intervals)
Failure modeling	Independent modes	Logic gates (AND/OR)	Impulse propagation (DMI)
Interdependencies	Poorly addressed	Difficult to model	Naturally represented via graph
Computational basis	Manual entry / tables	Boolean algebra	Python-based graph engine
Data format	Static docs / excel	Diagram files	Structured JSON / live stream
Decision support	Manual report analysis	Probabilistic estimation	Automated risk alerts
Risk metric	Risk priority number (RPN)	Failure probability	Structural/functional risk (R_s, R_f)

Analysis of Table 2 highlights the fundamental shift from document-centric reliability engineering (FMEA/FTA) to data-centric risk management (DT-CSM). The primary advantage of the proposed method lies in its computational basis and update frequency. While traditional methods rely on discrete, human-led audits, the DT-CSM engine operates autonomously in millisecond intervals. Furthermore, the transition from risk priority numbers (RPN) to a dual-metric approach (structural and functional risk) allows for a more nuanced understanding of system health. For instance, a high structural risk in a pipeline (e.g., the line to the engine GD) can be identified even if the individual pumps are functioning nominally, a scenario that is often overlooked in traditional independent-mode FMEA. This integration of real-time telemetry with graph-based impulse

modeling provides the necessary technological foundation for autonomous decision support systems in modern ship power plants. The transition to a DT-CSM framework enables the automation of decision-making. In emergency scenarios, while an FMEA report would be buried in documentation, the DT-CSM system provides the operator with an immediate visualization of the "at-risk" path (e.g., the critical line from F10 to GD), allowing for preventive intervention and mitigating the 40 % of failures typically associated with high-pressure fuel systems.

Conclusions and prospects for further research. The results of the study confirm the high efficiency of integrating DT technologies and cognitive simulation modeling, enabling automated risk assessment with a system response time within 50–100 ms, which meets the requirements for real-time control. The developed method for dynamic failure risk assessment ensured the identification of critical nodes in the SPP fuel system, where functional risk values reach 0.98 for the main engine (GD) and 0.91 for the circulation tank (F10), exceeding the criticality threshold of the Harrington scale (0.63) by 45 %. The practical value of the work is confirmed by the model's ability to identify "hidden risk zones" (0.37–0.63) for elements with partial degradation that are typically ignored by traditional binary FTA methods, while the presence of structural redundancy in the F11/FS11 pumps reduced local risk by 62 % compared to single lines. The use of the Python-based software package with an impulse convergence criterion of $\varepsilon=10^{-4}$ guarantees computational stability for graphs with more than 25 nodes, creating a foundation for reducing unplanned SPP downtime, 40 % of which is statistically linked to high-pressure fuel equipment failures. Prospects for future work involve expanding the model to other general ship systems, implementing neural network algorithms for the adaptation of importance coefficients β_i, and full integration of the developed "cognitive digital twin" into the onboard decision support systems of autonomous marine vessels.

REFERENCES

1. Vychuzhanin V., Vychuzhanin A. Intelligent diagnostics of ship power plants: Integration of case-based reasoning, probabilistic models, and ChatGPT. A universal approach to fault diagnosis and prognostics in complex technical systems : monograph. – Lviv–Torun : Liha-Pres, 2025. – DOI: https://doi.org/10.36059/978-966-397-516-0.

2. Vychuzhanin V., Vychuzhanin A. Dynamics of Failure Probabilities in Ship Power Plant Equipment Considering Cascade Effects // Вісник Східноукраїнського національного університету імені Володимира Даля. – 2025. – № 9(295). – С. 5–17. – DOI: https://doi.org/10.33216/1998-7927-2025-295-9-5-17.

3. V. Vychuzhanin and A. Vychuzhanin, "Integrated approach to creating a case-based database for diagnosing failures in ship power plants," *Informatics and Mathematical Methods in Simulation*, vol. 15, no. 2, pp. 155–165, 2025, https://doi.org/ 10.15276/imms.v15.no2.155.

4. Vychuzhanin V., Vychuzhanin A. Three-scenario analysis of fault diagnosis accuracy in complex technical systems. Information Technologies and Computer Engineering Vol. 22, No. 3. 2025. P23-40 https://doi.org/10.31649/vitce/3.2025.23.

5. Vychuzhanin V., Vychuzhanin A. Digital methods and models for control and survivability of complex technical systems : monograph. – Lviv–Torun : Liha-Pres, 2025. – 366 p. – DOI: https://doi.org/10.36059/978-966-397-556-6.

6. Qi Q., Tao F. Digital twin and big data towards smart manufacturing and Industry 4.0: 360-degree comparison // IEEE Access. – 2018. – Vol. 10. – P. 673–701. – DOI: https://doi.org/10.1109/ACCESS.2018.2793265.

7. Semeraro C., Lezoche M., Panetto H., Dassisti M. Digital twin paradigm: A systematic literature review // Computers in Industry. – 2021. – Vol. 130. – Article 103469. – DOI: https://doi.org/10.1016/j.compind.2021.103469.

8. Lv Z., Lv H., Fridenfalk M. Digital Twins in the Marine Industry // Electronics. – 2023. – Vol. 12, № 9. – Article 2025. – DOI: https://doi.org/10.3390/electronics12092025.

9. Leitão P., Colombo A. W., Karnouskos S. Industrial automation based on cyber-physical systems technologies: Prototype implementations and challenges // Computers in Industry. – 2015. – Vol. 81. – P. 11–25. – DOI: https://doi.org/10.1016/j.compind.2015.08.004.

10. Wagg D., Worden K., Barthorpe R., Gardner P. Digital Twins: State-of-The-Art Future Directions for Modelling and Simulation in Engineering Dynamics Applications // Mechanical Engineering Research. – 2020. – Vol. 6, № 3. – DOI: https://doi.org/10.1115/1.4046739.

11. Zio E., Miqueles L. Digital twins in safety analysis, risk assessment and emergency management // Reliability Engineering & System

Safety. – 2024. – Vol. 246. – Article 110040. – DOI: https://doi.org/10.1016/j.ress.2024.110040.

12. Ibrahim A., Kineber A. F., Mohandes S. R., Lan Y. et al. Understanding risk dynamics in digital twin integration: A causal analysis for smart infrastructure projects // Expert Systems with Applications. – 2026. – Vol. 297. – Article 129533. – DOI: https://doi.org/10.1016/j.eswa.2025.129533.

13. Qiu S., Zaheer Q., Ali F., Wajid S., Chen H., Ai C., Wang J. Exploring the impact of digital twin technology in infrastructure management: A comprehensive review // Journal of Civil Engineering and Management. – 2025. – Vol. 31, № 4. – P. 395–417. – DOI: https://doi.org/10.3846/jcem.2025.23718.

14. Li L., You J., Xu T. Risk analysis of digital twin project operation based on improved FMEA method // Systems. – 2025. – Vol. 13, № 1. – Article 48. – DOI: https://doi.org/10.3390/systems13010048.

15. Zhang X., Tao J., Noshadravan A. Probabilistic digital twin for reliability-based maintenance optimization of offshore wind turbines // Renewable Energy. – 2026. – Vol. 256. – Article 123777. – DOI: https://doi.org/10.1016/j.renene.2025.123777.

16. Wang Z., Wang Z. Risk Twin: Real-time risk visualization and control for structural systems // arXiv. – 2024. – Preprint arXiv:2403.00283. https://doi.org/10.48550/arXiv.2403.00283.

17. Li T., Bian Z., Lei H. et al. Digital Twin-based Driver Risk-Aware Intelligent Mobility Analytics for Urban Transportation Management // arXiv. – 2024. – Preprint arXiv:2407.15025. https://doi.org/10.48550/arXiv.2407.15025.

18. Tezzele M., Carr S., Topcu U., Willcox K. E. Adaptive planning for risk-aware predictive digital twins // arXiv. – 2024. – Preprint arXiv:2407.20490. https://doi.org/10.48550/arXiv.2407.20490.

19. Villegas W. Digital twin integration in metalworking: Enhancing efficiency and predictive maintenance // Frontiers in Mechanical Engineering. – 2025. – DOI: https://doi.org/10.3389/fmech.2025.1655565.

20. Homaei M., Mogollón-Gutiérrez Ó., Sancho J. et al. A review of digital twins and their application in cybersecurity based on artificial intelligence // Artificial Intelligence Review. – 2024. – Vol. 57. – Article 201. – DOI: https://doi.org/10.1007/s10462-024-10805-3.

21. Vychuzhanin V., Vychuzhanin A. Adequacy and verification of an intelligent diagnostic model for ship power plants // Informatics and

Mathematical Methods in Simulation. – 2025. – Vol. 15, № 3. – P. 312–326. – DOI: https://doi.org/10.15276/imms.v15.no3.312.

22. Madni A. M., Madni C. C., Lucero S. D. Leveraging digital twin technology in model-based systems engineering // Systems. – 2019. – Vol. 7, № 1. – Article 7. – DOI: https://doi.org/10.3390/systems7010007.

23. Hossain M. N., Rahman M. M., Ramasamy D. Artificial Intelligence-Driven Vehicle Fault Diagnosis to Revolutionize Automotive Maintenance: A Review // Computer Modeling in Engineering & Sciences. – 2024. – Vol. 141, № 2. – P. 951–996. – DOI: https://doi.org/10.32604/cmes.2024.056022.

24. Dalzochio J. et al. Machine learning and reasoning for predictive maintenance in Industry 4.0: Current status and challenges // Computers in Industry. – 2020. – Vol. 123. – Article 103298. – DOI: https://doi.org/10.1016/j.compind.2020.103298.